

MICROMECHANICAL STIFFNESS PREDICTIONS AT THE NANO-SCALE: CARBON NANOTUBE REINFORCED COMPOSITES

Eric J. Neer, Hsin-Piao Chen
California State University, Long Beach
1250 Bellflower Blvd
Long Beach, CA 90840

ABSTRACT

Nanotube reinforcement has the potential to provide significant mechanical improvement of polymer matrices. For three-phase composites (matrix/nanofiber/microfiber), this affords the opportunity to enhance off-axis properties dominated by the matrix. Before carbon nanotubes can be effectively used as a composite reinforcement, there must be a method of predicting stiffness gained from their use. Researchers have attempted to adapt micromechanical analyses (typically reserved for microfiber composites) to the nanoscale. One such model from Anumandla and Gibson (2006) accounts for nanotube orientation and waviness (ratio of amplitude to wavelength of assumed sinusoid) and relied upon the Chamis micromechanics equations. This is improved by implementing the Halpin-Tsai model, known for its accuracy at low reinforcement loadings, where nano-composites are typically fabricated. Extension to three-phase composites is done using laminated plate theory.

Micromechanical approaches are shown to be appropriate for use on the nano-scale (with proper considerations, identified in this work). Published experimental data for two-phase nano-composites is compared to the current model. Nanotube waviness is seen as a key parameter in composite stiffness. Modulus results agree well for waviness values within 10% and qualitatively agree with nano-composite SEM/TEM images. Three-phase data is limited, but initial comparisons show improvements in off-axis properties within a few percent.

1. INTRODUCTION

Many “micromechanical” models exist for the prediction of microfiber lamina stiffness. Several authors have attempted to extend these models to the nano scale for nanocomposite analysis. Herein is presented a review of the current work done toward this goal, with an analysis of the benefits and drawbacks of each. Nanotube form is identified as an important parameter in stiffness predictions due to the sensitivity of nanotube modulus to geometry. In addition to the nanotubes' form, three other factors are discussed which are necessary for reliable nanocomposite stiffness predictions. These are nanotube dispersion in the matrix, orientation effects, and waviness effects.

The Anumandla-Gibson (A-G) model is a micromechanical framework which is chosen for detailed analysis, discussion of sensitivities, and comparison with published experimental results. The original model makes use of C.C. Chamis' micromechanical equations for analyzing a representative volume element (RVE) consisting of matrix and nanotube. Since nanocomposites are generally fabricated at low nanotube volume fraction loadings, the A-G model is modified by

replacing the Chamis equations with the Halpin-Tsai equations, which are known to agree well with experimental results of microfiber composites. Using classical laminated plate theory, the present model is then extended to the realm of so called “three-phase” composites which use microfibers and a matrix reinforced with carbon nanotubes. Again comparisons are made to the published experimental results.

Good agreement is seen between the original and modified models and two-phase experimental data. However, the modified A-G model offers a smaller range of possible waviness values, which is important for several reasons. Three-phase composite data is limited to one data-set, but initial results are promising given that the present model predicts experimental results for unidirectional and quasi-isotropic laminates to within a few percent.

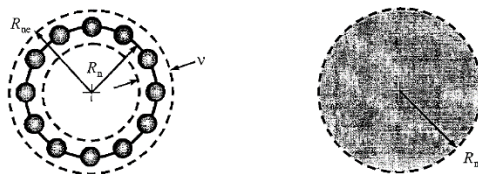
2. PROPERTIES OF CARBON NANOTUBES

2.1 Young’s Modulus, Geometry, and Density

For simplicity’s sake, it is tempting to assign a Young’s Modulus to a nanotube form for use in a micromechanical model, as is done with conventional microfibers. To this end, several studies have attempted to predict an elastic modulus for carbon nanotubes, but have reported a wide range of values. For example, Lourie and Wagner [1] give SWNT modulus values between 2.8 – 3.5 TPa and MWNT values between 1.7 – 2.4 TPa, whereas Sanchez et al. [2] and Yakobson and Avouris [3] report MWNT moduli being approximately 1 TPa and relatively independent of diameter. These and other large discrepancies are due in part to the authors treating nanotubes as they would a continuum, without careful consideration of their discrete nature.

Yakobson and Avouris [3] state that defining an elastic modulus implies a statistical spatial uniformity of the material. Since characteristic nanotube dimensions are on the same order as the dimensions of the carbon atoms that the tube is comprised of, there is a lack of “translational invariance” in the radial direction. Thus, a nanotube (whether SWNT, MWNT, or CNF) is not a *material*, but is more accurately an *engineering structure* [3]. Since CNTs must be treated as engineering structures, one cannot define an effective stiffness without taking into consideration the geometry of the CNT in question.

Pipes et al. [4] studied in-depth the intercorrelation between SWNT geometry, density, and tensile modulus by first considering the SWNT as a shell with thickness $\nu = 0.34nm$, the planar separation of graphite layers. Figure 1 (a) depicts the shell model and also shows the carbon atoms comprising the shell. The midplane radius, R_n , of the shell is a function of the nanotube’s chirality and the carbon-carbon bond length, 1.421 \AA [5]. With this information, the cross sectional area of the open cylinder can now be defined. This area is then assigned a modulus $E_n = 1029 \text{ GPa}$, the in-plane modulus of graphite.



a) Open cylinder model of SWCN

b) Filled cylinder model of SWCN

Figure 1: Open and Filled Cylinder Carbon Nanotubes [4]

The product of area and modulus of the open cylinder allows an effective *solid* cylinder (Figure 1 (b)) modulus to be defined through a simple scaling relation. The effective modulus of the solid cylinder will be less than that of the shell model, but the area-modulus product will be identical, i.e. (adapted from Thostenson and Chou [6]):

$$E_{solid} = \frac{A_{open}}{A_{solid}} E_{open}$$

This process yields *Figure 2*, where it can be seen that, depending on SWNT diameter, Young's modulus can vary drastically. A similar process and results are obtained for nanotube arrays, and one could extend the SWNT results to MWNTs by considering the added shell thickness from additional nanotubes.

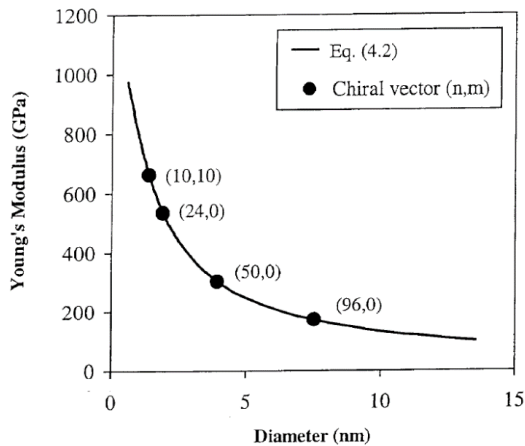


Figure 2: Nanotube Modulus vs Diameter [4]

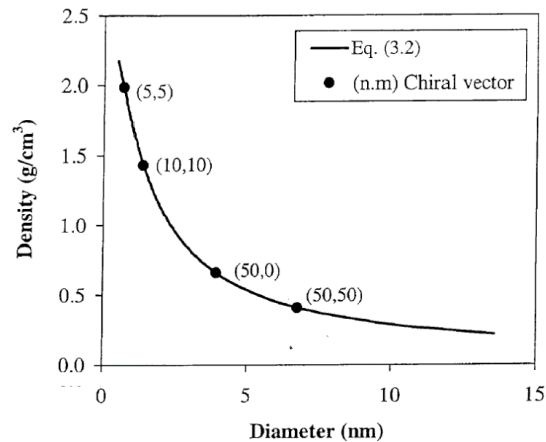


Figure 3: Nanotube Density vs Diameter [4]

With nearly all micromechanical models, the volume fraction of the reinforcement in the composite is used. However, as will be seen later, a majority of experimental work done with CNTs provide loadings in terms of weight. This necessitates a definition of a density to allow conversion from weight to volume. The same arguments and complications for defining a Young's Modulus apply to defining a density. Pipes et al [4] also tackles this discrepancy through a process similar to that described above except instead of assigning a modulus to the open cylinder, a mass is assigned, namely the mass of the carbon atoms comprising the shell. The mass is then assumed to occupy the volume of the solid cylinder, giving an effective density. Figure 3 shows the result of this exercise.

Figure 2 and Figure 3 clearly indicate the sensitivity of nanotube properties to its geometry, thus any attempt to predict CNT reinforcing capabilities in two of three-phase composites must be with consideration of nanotube geometry.

2.2 Carbon Nanotube Reinforced Composites

Carbon nanotubes possess, mechanical, thermal, and electrical properties which are equal or superior to any current materials which makes them an attractive candidate for enhancing a variety of matrices. They would offer immediate benefits in structures which cannot accommodate conventional reinforcement, such as polymer fibers, foams, and films [7]. Their added benefit extends to conventional carbon fiber reinforced polymer composites (CFRPs) as well. CFRPs generally suffer from poor properties in off-fiber directions where material characteristics are dominated by matrix properties [8].

There are four topics which any micromechanical model must address when predicting reinforcement capability of a CNT reinforced matrix [9] [10] [11].

1. *Dispersion/Agglomeration of CNTs.* Nanotubes and other nano-reinforcements exhibit exceptionally high surface area to volume ratios compared to conventional reinforcements (see Figure 4) While beneficial to interfacial stress transfer, this large surface area also causes CNTs to have a strong tendency to bundle together to form agglomerations, which can act as defects in a two or three-phase composite [12]. Usually in micromechanical analyses, the assumption of uniform dispersion is made.

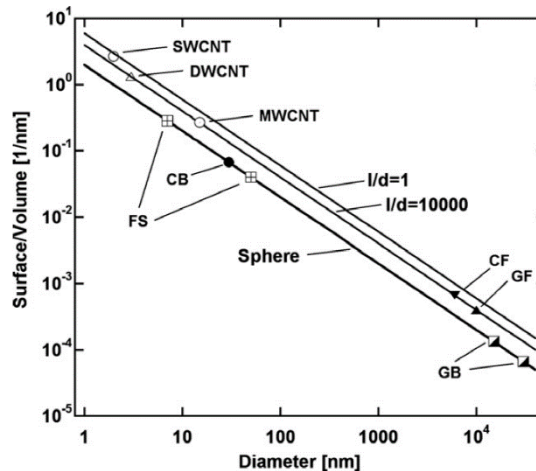


Figure 4: Surface/Volume vs Diameter for Different Reinforcement [12]

2. *Orientation.* CNTs have been shown to be highly anisotropic, with off axis properties being an order of magnitude less than on axis [13] [14]. If nanotubes tend to orient in one direction more than others (as was done in Thostenson and Chou [6] and Mora et al. [15] through a drawing process), their anisotropy may be transferred to the composite.
3. *Length and Aspect Ratio.* Microfiber length has been shown to be an important parameter for conventional composites for decades. Coleman et al. [11] present both a modified rule-of-mixtures and the Halpin-Tsai micromechanical models with incorporate length efficiency parameters. The general rule is that, the longer the fiber is, the more efficient it is due to an increased area available for stress transfer from the matrix to the fiber. This is expected to apply to nanotube reinforcements as well.

4. *Waviness*. Relatively little work has been done to model the effects tube waviness has on mechanical properties of CNT reinforced composites [9] [16] [17] [18]. It is common to see micromechanical approaches that consider CNTs straight to simplify analyses [19] [20] [10] [21] [22] [23]. This simplification, however, usually leads to an overestimation of predicted stiffness due in large part to the fact that nanotubes are decidedly not straight in experimental settings (without special process to encourage alignment, e.g. drawing). Figure 5 is a TEM image of MWNTs dispersed in a polystyrene matrix where one can see the varying degrees of curvature. This waviness degrades the reinforcing capabilities of CNTs and thus must be accounted for.

Interfacial shear strength between the fiber (whether CNF or microfiber) and matrix is an important parameter in the normal use of composites, but less so when making stiffness predictions. The perfect bonding assumption is made, and for low strain conditions, this assumption is valid.

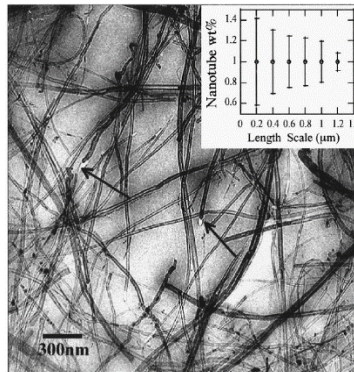


Figure 5: MWNTs Dispersed in Polystyrene Matrix [24]

3. MODIFIED ANUMANDLA-GIBSON MODEL

A summary of the Anumandla-Gibson model is presented here. For an in-depth development of the model, the reader is directed to the original publication of the model [16]. Modifications to the model are presented in detail with justification and ramifications of each. Extension of either model to three-phase composites is done using classical laminated plate theory and the Halpin-Tsai micromechanics equations. Details of these can be found in the thesis that served as the basis of the present work [25] or any other text on composites analysis.

3.1 Anumandla-Gibson

The Anumandla-Gibson model uses a two-RVE approach, as depicted in Figure 6. The first step in the process is to estimate the properties of RVE1 and the Chamis [26] micromechanics equations are used for this. At this point it is assumed that the fiber is straight, isotropic, and since it spans the entire RVE, continuous. With knowledge of RVE1 properties, RVE1 compliances (for a zero-fiber-waviness condition) can be calculated. The assumption of a thin, unidirectional lamina under plane stress is made in doing this.

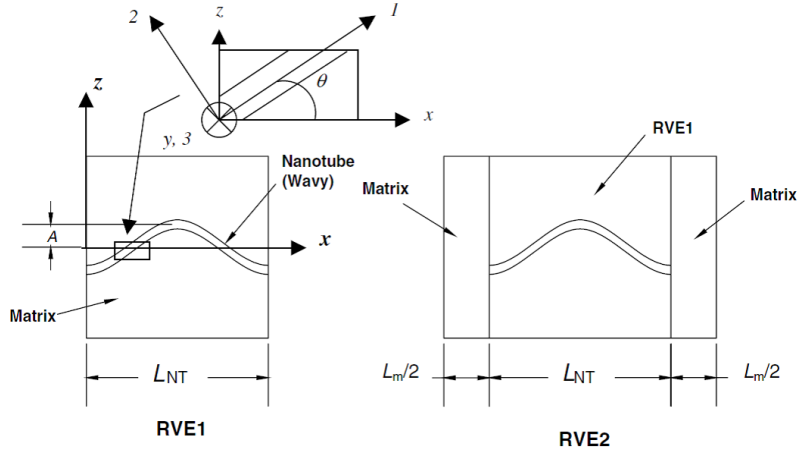


Figure 6: Representative Volume Element (RVE) Used in Anumandla-Gibson

Effects of fiber waviness are included through use of Hsaio and Daniel's [27] model where an RVE similar to that of RVE1 is used. This RVE is sliced in to infinitesimal pieces of width dx . Each slice is treated as an off-axis lamina whose properties may be calculated using standard micromechanical approach and transformed with the standard transformation matrix. Averaging the strains over one wavelength and having knowledge of the applied stresses allows calculation of *effective* (i.e. with waviness) properties.

Waviness is quantified through a so called "wavy factor" which is the ratio of the amplitude of the nanotube (A in Figure 6) to the length of RVE1 (L_{NT} in Figure 6). Wavy factors of 0, 5, 10, 25, and 50% are used in modulus vs volume fraction plots to be shown. Orientation effects are accounted for through the model of Christensen and Waals [38], with RVE1 strains being averages over all possible orientations of the nanotube. Finally, an effective modulus for RVE2 is computed through an inverse rule of mixtures using matrix and RVE1 regions of RVE2. The result of this process yields an isotropic modulus of RVE2.

3.2 Modification

3.2.1 Micromechanical Model in RVE1

In the Anumandla-Gibson model, there are actually two sets of micromechanical equations that are used. The Chamis equations are used to predict RVE1 properties, and an inverse rule of mixtures is used to predict RVE2 properties. It is not immediately clear how appropriate the Chamis equations are for use here, so they were replaced by the Halpin-Tsai equations to gauge if either has an advantage over the other. The Halpin-Tsai equations, for microfiber composites, are known to fit experimental data well at low volume fractions [11]. Since CNT composites are almost exclusively fabricated at low loadings ($\leq 10\%$), the Halpin-Tsai model may show improvement over the chamis model.

The generalized Halpin-Tsai model is as follows [28]:

$$\frac{\bar{P}_c}{P_m} = \frac{1 + \zeta\eta v_f}{1 - \eta v_f}$$

P_c is a composite property (E_{22} , G_{12} , or ν_{23}) and P_m or P_f is the corresponding matrix or fiber property. ζ is a measure of reinforcement and depends on boundary conditions. Generally accepted values used for ζ are:

Property	ζ	Reference
E_{22}	2	[28]
G_{12}	$1 + 40 \nu_f^{10}$	[29]
ν_{23}	1	

For E_{11} and ν_{12} , ζ takes on a very large value for continuous fiber composites. In the limit as $\zeta \rightarrow \infty$, the Halpin-Tsai equations reduce to the rule of mixture. Thus, the rule of mixture is used in calculation of these properties.

Figure 7 shows the result of this exercise. It can be seen for zero waviness, the two models produce identical results, which is expected. However, with increasing waviness, the Halpin-Tsai model shows a quicker reduction in modulus. At sufficiently low loadings and high waviness, the Halpin-Tsai equations actually predict a *reduction* in modulus. Section 4 will compare both the Chamis and Halpin-Tsai predictions to experimental results.

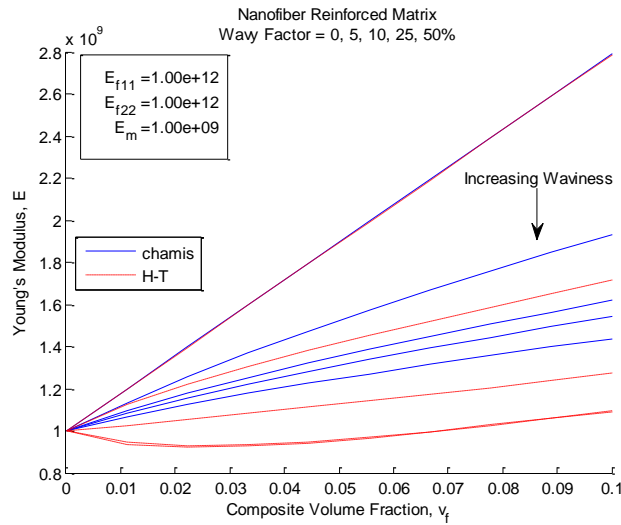


Figure 7: Halpin-Tsai and Chamis Models in RVE1 Results

3.2.2 Isotropic vs Transversely Isotropic CNFs

One of the key simplifying assumptions made in the A-G model is that the embedded nanotube is isotropic. Though, as was previously mentioned in section above 2.1, nanotubes are decidedly *not* isotropic. It is desired to see how large of an impact this assumption has on model predictions.

The Chamis and Halpin-Tsai micromechanical models are able to handle transversely isotropic reinforcement, so no modification of the equations is necessary. What is needed are representative off-axis nanotube properties, and Table 1 gives values selected for simulation.

Table 1: Transversely Isotropic CNT Properties

Property	Value	Reference
E_{11}	1 TPa	[30] ((9,0) High AR Uncapped)
E_{22}	68.3 GPa	[13]
G_{12}	0.37 TPa	[31] (1 CNT wall torsion test)
ν_{12}	0.3	[16]
ν_{23}	0.34	[13]

Figure 8 and Figure 9 depict predictions using an isotropic and a transversely isotropic fiber. The difference between the plots is negligible. For example, at 5% waviness and 25% volume fraction each model predicts values shown in Table 2.

Table 2: RVE2 Sample Results for Isotropic and Transversely Isotropic CNFs (5% waviness, 25% volume fraction)

Model	Case	
	Isotropic	Transversely Isotropic
Chamis	2.987 GPa	2.981 GPa
Halpin-Tsai	2.643 GPa	2.629 GPa

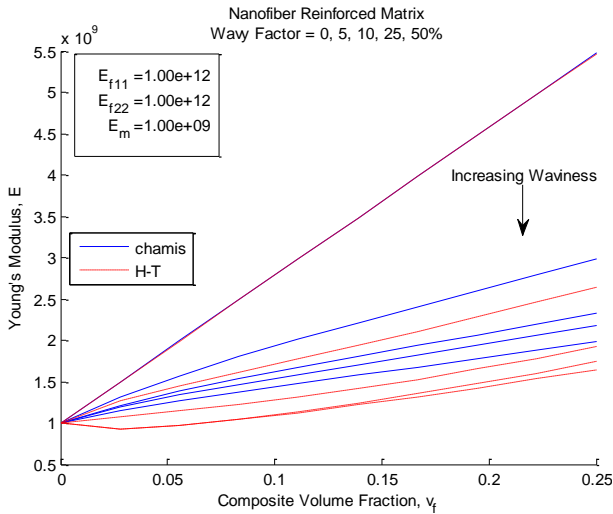


Figure 8: Waviness Plot with Isotropic Nanofiber

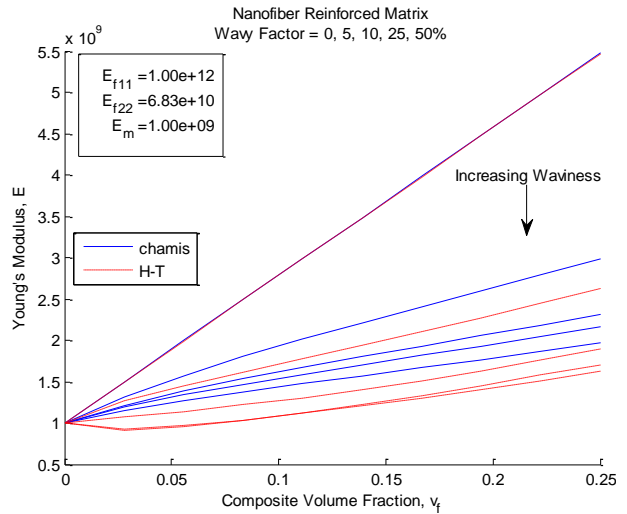


Figure 9: Waviness Plot with Anisotropic Nanofiber

Similar results are seen for other volume fractions and waviness values. These suggest that considering a fiber to be isotropic is a good assumption for this model. This is likely due to nanofibers being assumed to be uniformly dispersed and randomly oriented, along with the fact that primary stiffness contributions come from the nanotube's exceedingly high tensile modulus.

4. COMPARISON WITH EXPERIMENTAL RESULTS

4.1 Two-Phase Composites

In the original publication of the A-G model, Anumandla [16] compared model predictions to published experimental results from Andrews et al [32]. This comparison was recreated in Figure 10 to ensure MATLAB implementation matched results from the original publication, and to additionally compare results using the Halpin-Tsai modification.

Good agreement is seen between experimental and theoretical results, but this is limited to one dataset. A literature survey was done to collect additional results for comparison, the results of which are shown in Figure 11 through Figure 16. All plots show moduli of fiber and matrix.

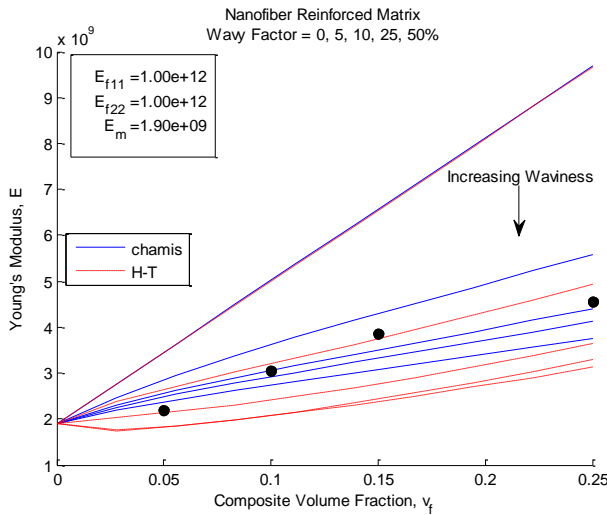


Figure 10: Andrews et al Experimental Data with A-G and Current Models

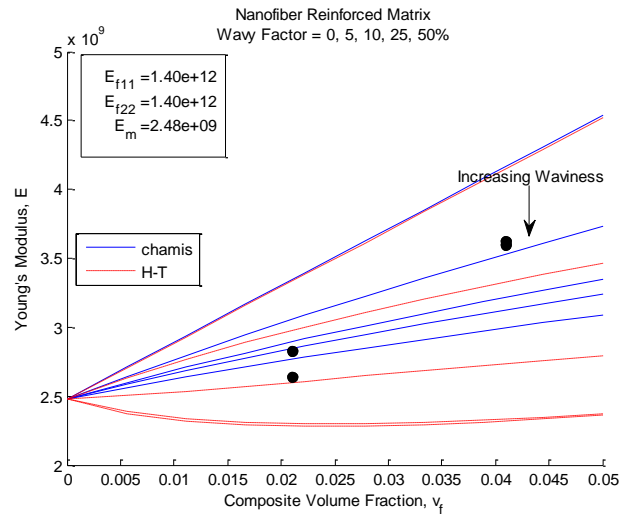


Figure 11: Iwahori Experimental Data

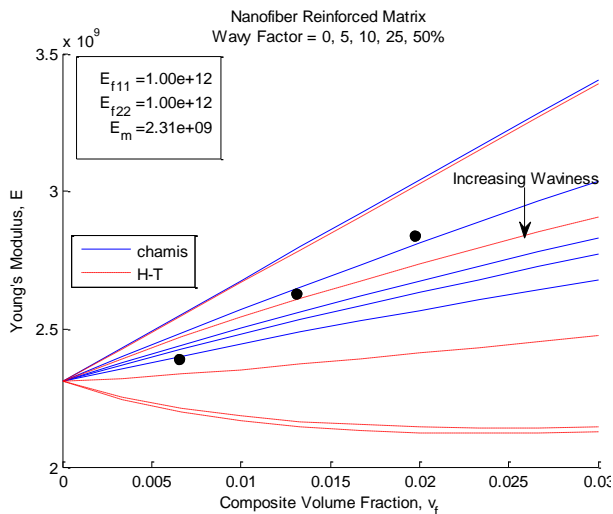


Figure 12: Zhou Experimental Data (0.02/s strain rate)

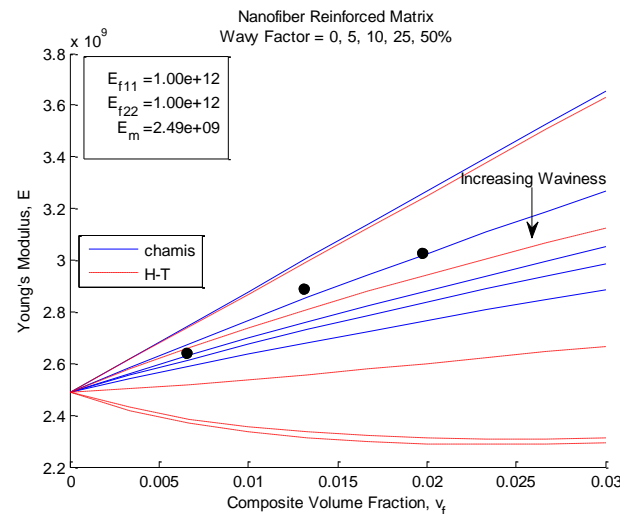


Figure 13: Zhou Experimental Data (0.2/s strain rate)

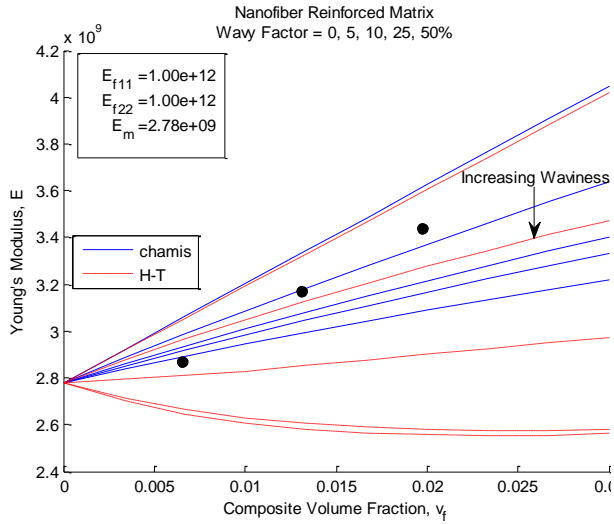


Figure 14: Zhou Experimental Data (2/s strain rate)

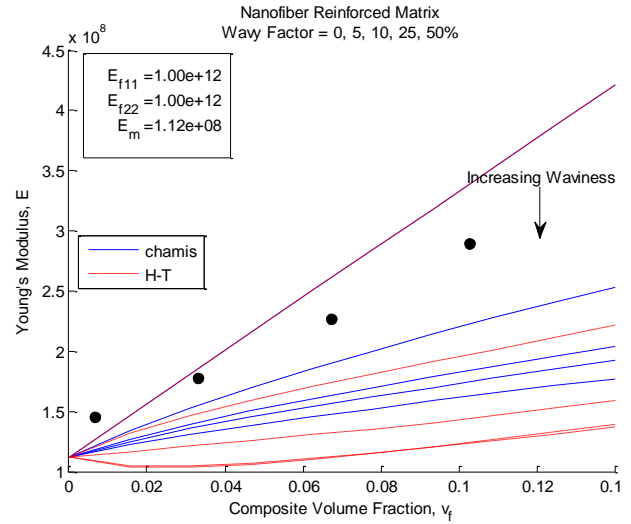


Figure 15: Ogale Experimental Data

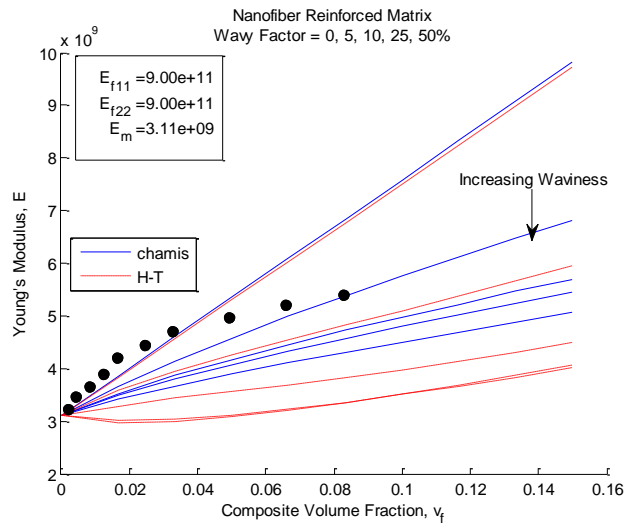


Figure 16: Omidi Experimental Data

On reviewing the plots generated comparing experimental and model results, several trends can be identified. For the Chamis implementation, a decent portion of experimental results lie between 5-25% waviness, which agrees well with Anumandla's [16] original conclusion. For the Halpin-Tsai model, nearly all experimental results lie between 0 and 10% waviness lines, which gives a narrower band of waviness values than does the Chamis model. Having this small band of lower waviness values is important since, as discussed in subsection 3.1.1, higher wavy factors violate transverse isotropy more. To add to this, 0 and 10% waviness seems more realistic given the high aspect ratios typical of nanotubes. Some experimental results agree with the 25 and 50% wavy factor lines of the Chamis implementation. In reality, with nanotube lengths being on the order of millimeters, this could mean the wavy amplitude is several hundred diameters. This qualitatively does not agree with Figure 5 or other SEM/TEM nanocomposite images seen in literature.

Omidi et al [33] had the most outlying data points. Below volume fractions of about 4%, experimental values followed the trend of the 0% waviness lines, but at slightly higher modulus values. Data for volume fractions between 4 and 10% fell in between the 0 and 5% waviness lines of each model. A possible explanation for this is the method of manufacture of the test specimen used in the study. Test coupons were fabricated through casting in this case. Depending on the flow in to the mold, there could have been some bias towards a particular direction in alignment of nanotubes. The authors also state that samples were mechanically polished prior to testing. Thostenson and Chou [19] prepared MWNT/Polystyrene samples using a microtome cutting process and reported distortion of the nanotubes in the cutting direction, meaning the cutting process influenced tube alignment. Details are not given on the mechanical polishing of Omidi et al. but if polishing were done along one direction it could again make the nanotubes tend along the cutting plane, which would violate the random alignment assumption.

4.2 Three-Phase Composites

Relatively little experimental work has been published regarding three-phase composites. Two works were reviewed which reported experimental data for nanotube reinforced hierarchical composites. Yokozeki et al. [34] was the only article reviewed which prepared three-phase composites using unidirectional fibers. Carbon fiber prepreps were developed using resin infused with 5 and 10% by weight cup-stacked carbon nanotubes. Cup-stacked nanotubes are a special form of the MWNT, where each layer has been rolled up in to a conical shape rather than a tube. Unidirectional and quasi-isotropic laminates were fabricated and tested.

Since unidirectional fibers were used, the laminates can be analyzed using the current micromechanical model in combination with classical laminated plate theory. T700SC-12K fibers were used in combination with EP827 epoxy (Japan Epoxy Resin Co.) for the prepreg material. Detailed material data for these constituents was not readily available. T-300 Carbon Fiber and HY6010 epoxy properties were substituted for analysis, and comparisons between experiment and theory can be drawn by examining the *relative change* in properties over the baseline 0% laminate.

Table 3 and Table 4 compare experimental results with predicted values. Changes over baseline 0% CNF laminates are shown in parentheses. Fiber volume fraction for each laminate was nominally 65% with a ply thickness of 0.125mm. A waviness value of 10% was assumed for nanotubes.

Regarding the unidirectional laminate, experimental on-axis stiffnesses between the neat and CNF reinforced composite were statistically identical (standard deviation of 2.0 for tensile measurements). The current model predicts negligible increases in tensile stiffness. These results are expected because on-axis properties are dominated by the microfiber in the composite. Transverse experimental stiffness showed an appreciable increase of almost 6% over the baseline. The work presented here slightly under-predicts experimental results.

For the quasi-isotropic laminate, results were under-predicted by a larger margin. The largest discrepancy is seen with the 5% case, where predicted increase in modulus is around 1% whereas experimental increase was 3%. CNTs could be doing more than just making the matrix material stiffer. If they are improving the transfer of stress from the matrix to the microfibers it could result in a higher composite modulus. The assumption of 10% waviness in the nanofiber may also be too high, which would quickly degrade predicted modulus. Section 4.1 showed experimental often fell somewhere between 0-10% waviness.

It is interesting to note that doubling the weight fraction of nanotubes from 5 to 10% (which in this case is roughly equivalent to doubling volume fraction) in experiment resulted in only an additional 0.9% increase of stiffness. This could suggest that loading and stiffness in the 0-10% loading range have a non-linear relationship. Figure 16 had the largest experimental data set for two-phase composites and exhibits just such a non-linear response in this region.

Table 3: Three-Phase Composite Results (Experimental and Theoretical) $[0]_{16}$ Unidirectional Laminate, GPa

Source	0% Weight		5% Weight	
	0° Stiffness	90° Stiffness	0° Stiffness	90° Stiffness
Experiment [34]	131	8.61	129 (-1.5%)	9.11 (+5.8%)
Present Model + CLPT	150.7	8.793	150.8 (--)	9.143 (+4.0%)

Table 4: Three-Phase Composite Results (Experimental and Theoretical) $[0/90/+/-45]_{35}$ Quasi-Isotropic Laminate, GPa

Source	0% Weight	5% Weight	10% Weight
Experiment [34]	46.5	47.9 (+3.0%)	48.3 (+3.9%)
Present Model + CLPT	57.8	58.3 (+0.9%)	58.7 (+1.6%)

5. CONCLUSIONS

In this work, an existing micromechanical model (Anumandla-Gibson) for analysis of carbon nanotube reinforced composites was modified by replacing its usage of the Chamis equations with that of the Halpin-Tsai equations since they are known to yield good approximations at low volume fractions. The model was then extended to three-phase composites using classical laminated plate theory.

Two-phase predictions showed promising results when compared with experimental results from literature. Waviness values between 0 and 10% for the Halpin-Tsai model agree best with experiment. Three-phase results tended to under-predict improvement with nanotube loading,

which may suggest another mechanism is at play or assumed waviness values were not representative of experimental values.

One of the severely limiting aspects of experimental results thus far is a rigorous definition of geometry used. As was shown, this geometry determines key properties of the nanotube. This presents an issue because unlike microfibers which have relatively consistent geometry, nanotube lengths, diameters, and thicknesses are not single valued due to how they are manufactured. By extension then, there would not be a single value for nanotube modulus. Improvement to the current model can be made with comparison to experimental results that also took note of the geometry of nanotubes used.

Like nanotube geometry, nanotube “waviness” is not, in reality, a single value. The current model suggests waviness values between 0 and 10% are reflective of reality. However, without SEM/TEM images like that of Figure 5, this cannot be said for sure. If one is to include effects of waviness, then more images like this one are necessary to gauge degrees of waviness in experiment.

6. REFERENCES

- [1] O. Lourie and W. H. D., "Evaluation of Young's modulus of carbon nanotubes by micro-Raman spectroscopy," *Journal of Materials Research*, pp. 2418-2422, 2009.
- [2] D. Sanchez-Portal, E. Artacho, J. M. Soler, A. Rubio and P. Ordejón, "Ab initio structural, elastic, and vibrational properties of carbon nanotubes," *Physical Review B*, vol. 59, no. 19, pp. 12678-12688, 1999.
- [3] B. I. Yakobson and P. Avouris, "Mechanical properties of carbon nanotubes," in *Topics in Applied Physics*, 2001, pp. 287-327.
- [4] R. Pipes, S. J. V. Frankland, P. Hubert and E. Saether, "Self-consistent physical properties of carbon nanotubes in composite materials," NASA Langley Research Center, Hampton, VA, 2002.
- [5] M. Dresselhaus, G. Dresselhaus and R. Saito, "Physics of carbon nanotubes," *Carbon*, vol. 33, no. 7, pp. 883-891, 1995.
- [6] E. T. Thostenson, W. Z. Li, D. Z. Wang, Z. F. Ren and T. W. Chou, "Carbon nanotube/carbon fiber hybrid multiscale composites," *Journal of Applied physics*, vol. 97, no. 9, pp. 6034-6037, 2002.
- [7] H. Qian, E. S. Greenhalgh, M. S. Shaffer, S. Milo and A. Bismarck, "Carbon nanotube-based hierarchical composites: a review," *Journal of Materials Chemistry*, vol. 20, no. 23, pp. 4751-4762, 2010.
- [8] M. Tehrani, A. Y. Boroujeni, T. B. Hartman and T. P. C. S. W. A.-H. M. Haugh, "Mechanical characterization and impact damage assessment of a woven carbon fiber reinforced carbon nanotube–epoxy composite," *Composites Science and Technology*, vol. 75, pp. 42-48, 2013.
- [9] F. T. Fisher, R. D. Bradshaw and L. C. Brinson, "Effects of nanotube waviness on the modulus of nanotube-reinforced polymers," *Applied Physics Letters*, vol. 80, no. 24, pp. 4647-4649, 2002.

- [10] M. Griebel and J. Hamaekers, "Molecular dynamics simulations of the elastic moduli of polymer-carbon nanotube composites," *Computer methods in applied mechanics and engineering*, vol. 193, no. 17, pp. 1773-1788, 2004.
- [11] J. N. Coleman, U. Khan, W. J. Blau and Y. K. Gunko, "Small but strong: a review of the mechanical properties of carbon nanotube-polymer composites," *Carbon*, vol. 44, no. 9, pp. 1624--1652, 2006.
- [12] B. Fiedler, F. H. Gojny, M. H. Wichmann, M. C. Nolte and K. Schulte, "Fundamental aspects of nano-reinforced composites," *Composites science and technology*, vol. 66, no. 16, pp. 3115-3125, 2006.
- [13] E. Saether, S. J. V. Frankland and R. B. Pipes, "Transverse mechanical properties of single-walled carbon nanotube crystals. Part I: determination of elastic moduli," *Composites Science and Technology*, vol. 63, no. 11, pp. 1543-1550, 2003.
- [14] D.-L. Shi, X.-Q. Feng, Y. Y. Huang, K.-C. Hwang and H. Gao, "The effect of nanotube waviness and agglomeration on the elastic property of carbon nanotube-reinforced composites," *Journal of Engineering Materials and Technology*, vol. 126, no. 3, pp. 250-257, 2004.
- [15] R. J. Mora, J. J. Vilatela and A. H. Windle, "Properties of composites of carbon nanotube fibres," *Composites Science and Technology*, vol. 69, no. 10, pp. 1558-1563, 2009.
- [16] V. Anumandla and R. F. Gibson, "A comprehensive closed form micromechanics model for estimating the elastic modulus of nanotube-reinforced composites," *Composites Part A: Applied Science and Manufacturing*, vol. 37, no. 12, pp. 2178-2185, 2006.
- [17] L. H. Shao, R. Y. Luo, S. L. Bai and J. Wang, "Prediction of effective moduli of carbon nanotube-reinforced composites with waviness and debonding," *Composite structures*, vol. 87, no. 3, pp. 274-281, 2009.
- [18] K. Yanase, S. Moryama and J. W. Ju, "Effects of CNT waviness on the effective elastic responses of {CNT}-reinforced polymer composites," *Acta Mechanica*, vol. 224, no. 7, pp. 1351-1364, 2013.
- [19] E. T. Thostenson and T.-W. Chou, "Aligned multi-walled carbon nanotube-reinforced composites: processing and mechanical characterization," *Journal of physics D: Applied physics*, vol. 35, no. 16, 2002.
- [20] S. Kanagaraj, F. R. Varanda, T. V. Zhiltsova, M. S. Oliveira and J. A. Simes, "Mechanical properties of high density polyethylene/carbon nanotube composites," *Composites Science and Technology*, vol. 67, no. 15, pp. 3071-3077, 2007.
- [21] G. M. Odegard, T. S. Gates, K. E. Wise, C. Park and E. J. Siochi, "Constitutive modeling of nanotube-reinforced polymer composites," *Composites science and technology*, vol. 63, no. 11, pp. 1671-1687, 2003.
- [22] X. L. Chen and Y. J. Liu, "Square representative volume elements for evaluating the effective material properties of carbon nanotube-based composites," *Computational Materials Science*, vol. 29, no. 1, pp. 1-11, 2004.
- [23] G. D. Seidel and D. C. Lagoudas, "Micromechanical analysis of the effective elastic properties of carbon nanotube reinforced composites," *Mechanics of Materials*, vol. 38, no. 8, pp. 884-907, 2006.

- [24] D. Qian, E. C. Dickey, R. Andrews and T. Rantell, "Load transfer and deformation mechanisms in carbon nanotube-polystyrene composites," *Applied Physics Letters*, vol. 76, no. 20, pp. 2868-2870, 2000.
- [25] E. Neer, "Stiffness predictions of carbon nanotube reinforced two and three-phase polymer composites," ProQuest Open, Long Beach, CA, 2015.
- [26] C. C. Chamis, "Simplified composite micromechanics equations of hygral, thermal, and mechanical properties," *SAMPE Quarterly*, vol. 15, pp. 14-23, 1984.
- [27] H. M. Hsiao and I. M. Daniel, "Elastic properties of composites with fiber waviness," *Composites Part A: Applied Science and Manufacturing*, vol. 27, no. 10, pp. 931-941, 1996.
- [28] J. C. Halpin, "Effects of Environmental Factors on Composite Materials," DTIC Document, 1969.
- [29] R. M. Jones, *Mechanics of composite materials*, New York: McGraw-Hill, 1975.
- [30] X.-L. Gao and K. Li, "A shear-lag model for carbon nanotube-reinforced polymer composites," *International Journal of Solids and Structures*, vol. 42, no. 5, pp. 1649-1667, 2005.
- [31] A. Ghavamian, M. Rahmandoust and A. Öchsner, "On the determination of the shear modulus of carbon nanotubes," *Composites Part B: Engineering*, vol. 44, no. 1, pp. 52-59, 2013.
- [32] R. Andrews, D. Jacques, M. Minot and T. Rantell, "Fabrication of carbon multiwall nanotube/polymer composites by shear mixing," *Macromolecular Materials and Engineering*, vol. 287, no. 6, pp. 395-403, 2002.
- [33] M. Omid, H. R. DT, A. S. Milani, R. J. Seethaler and R. Arasteh, "Prediction of the mechanical characteristics of multi-walled carbon nanotube/epoxy composites using a new form of the rule of mixtures," *Carbon*, vol. 48, no. 11, pp. 3218-3228, 2010.
- [34] T. Yokozeki, Y. Iwahori, S. Ishiwata and K. Enomoto, "Mechanical properties of {CFRP} laminates manufactured from unidirectional prepregs using CSCNT-dispersed epoxy," *Composites Part A: Applied Science and Manufacturing*, vol. 38, no. 10, pp. 2121-2130, 2007.
- [35] A. Y. Boroujen, M. Tehrani, A. J. Nelson and A.-H. M., "Hybrid carbon nanotube/carbon fiber composites with improved in-plane mechanical properties.," *Composites Part B: Engineering*, vol. 66, pp. 475-483, 2014.
- [36] Y. Zhou, S. Jeelani and T. Lacy, "Experimental study on the mechanical behavior of carbon/epoxy composites with a carbon nanofiber-modified matrix," *Journal of Composite Materials*, 2013.
- [37] Y. Iwahori, S. Ishiwata, T. Sumizawa and T. Ishikawa, "Mechanical properties improvements in two-phase and three-phase composites using carbon nano-fiber dispersed resin," *Composites Part A: Applied Science and Manufacturing*, vol. 36, no. 10, pp. 1430-1439, 2005.
- [38] A. Ogale, S. Lee and M.-S. Kim, "Influence of carbon nanofiber structure on polyethylene nanocomposites," *Plastics Research Online*, 2010.